

# Activities of Superconducting Cavity for KEK B-Factory

S.Mitsunobu,K.Asano,T.Furuya,Y.Ishi\*,Y.Kijima\*,K.Ohkubo\*\*,  
T.Tajima and T.Takahashi

National Laboratory for High Energy Physics

1-1 Oho, Tsukuba-shi,Ibaraki-ken,305,Japan

\* Mitsubishi Electric Corporation

\*\* Mitsubishi Heavy Industries,LTD.

## 1. Introduction

KEK B-Factory is an asymmetric-energy electron- positron collider to detect the CP violation of B-mesons. If the Kobayashi-Masukawa model is a correct description of nature, we can expect sizable CP-violation effect in several B-meson decay channels ; however,the branching ratio of the decay channels are rather small and we should have a collider with  $2 \sim 10 \times 10^{33} \text{ cm}^{-2}\text{s}^{-1}$  luminosity[1]. The luminosity goal of the KEK B-Factory is  $10^{34} \text{ cm}^{-2}\text{s}^{-1}$ , which will be storing 2.6 A in the low-energy (positron) ring (LER) and 1.1 A in the high-energy (electron) ring (HER). The KEK B-Factory,named TRISTAN II, will be constructed in existing TRISTAN tunnel. In start of the B-Factory,normal conducting cavities and four superconducting cavities will be installed to accelerate beams.

Before B-Factory operation ,a beam accumulation test of 0.5 A is also scheduled in 1995 in TRISTAN Accumulation Ring (AR) together with normal conducting damped cavities.

Table 1 summarizes the parameters of the superconducting cavity system for KEK B-Factory and that of AR test.

Table 1 Main parameters of SC cavity for KEK B-Factory and AR test

	LER	HER	AR test	
Energy	3.5	8.0	2.5	GeV
RF voltage	22	48	2.5	MV
Beam Current	2.6 (0.52)	1.1 (0.22)	0.5	A
R/Q	93	93	9	Ohm
$Q_0$	$2 \times 10^9$	$2 \times 10^9$	$2 \times 10^9$	
$Q_L$	$2 \times 10^5$	$2 \times 10^5$	$2 \times 10^5$	
Number of cells	10 (2)	20 (2)	1	
Voltage/cell	2.2	2.4	2.5	MV
Eacc	9.1	9.9	10.3	MV/m
Power/cell	250	240	140	kW

## 2. Superconducting Cavity and Cryostat

For a large current of 2.6 A, we adopted a single cell superconducting cavity to reduce the input coupler load and HOM load.

A concept of HOM damping is to extract HOM power out of the cavity and absorb the power by ferrite absorbers attached to the inner surface of the beam pipe. The shape of the cell and the beam pipe should make the  $Q_{ext}$  of all HOM's low enough to couple out to the beam pipes. If the property of ferrite is good enough, it is expected that  $Q_i$  of all HOMs are approximately equal to  $Q_{ext}$ . In Cornell University, a cavity with a "fluted" beam pipe has been studied [2]. In KEK, after Cu model cavity test [3], we adopted a large diameter beam pipe because of the ease of manufacturing under regulation of high pressure cord.

The geometry of the cavity is shown in Fig. 1. One of the beam pipes has a large diameter of 30 cm (large beam pipe; LBP) which is optimized so as to lower the cut off frequency than that of HOM's. The diameter of the other beam pipe is 22 cm (small beam pipe; SBP). HOM power is damped by ferrite which are located on the inner surface of the beam pipes. The geometry of superconducting cavity is designed so that the external  $Q$ 's of HOM's become as small as possible [4]. The parameters of HOM damper such as thickness, length and position have been studied on TDK ferrite IB-004 by SEAFISH program that was transferred from Cornell University. An aluminum model cavity was manufactured to check the design properties [5].

The cryostat design based on the TRISTAN cavity cryostat [6] started for the AR test cavity. Fig. 2 shows the structure of the cryostat. SBP is fixed to He vessel and LBP is moved by a tuner which is set on the out side of the vacuum vessel.

The mechanical property of the cavity was studied. The required property of niobium is fixed, like as yield strength should be higher than  $10 \text{ kg/mm}^2$  and RRR higher than 150.

The construction of AR test cavity and cryostat starts this year and will be finish till Fy 1994.

## 3. Vertical Test of Nb Prototype Cavity

A prototype cavity was fabricated and measured [4]. Fig. 3 shows  $Q_0$ -Eacc curves. 19 X-ray sensors and 25 carbon resistors were distributed on a frame along one meridian of outer surface between the lower and upper irises. Rotating speed of the frame was controlled by the sensor position controller in 2~6 minutes per turn, and it took about 2 seconds to scan all channels of the sensor arrays. The data were taken at every 2-6 degree. Fig. 4 (a)-(d) show the temperature-rise maps and X-ray maps of the first measurement at each field level. In the first measurement, the  $Q_0$  dropped suddenly from  $1.22 \times 10^9$  to  $5.42 \times 10^8$  at Eacc = 10 MV/m. For recovering the  $Q_0$ , we tried RF-processing of about 75 minutes, but the cavity performance did not change. At this field, the X-ray map showed the large peak near the lower iris on the meridian of 45 degree and temperature map also showed the heating spot at the same position (Fig. 4(a)). Next we tried pulse aging (~200W, several msec) for 120 minutes and the performance of the cavity could be recovered. During the pulse aging, temperature map showed the large heating spot

on the 150 degree meridian instead of the spot on the 45 degree. Fig. 4(b) shows the maps during the pulse aging process and the maps just after the aging is in Fig. 4(c) at the field of 9.4 MV/m. This means that the degradation of the  $Q_0$  was caused by the electron emission on the meridian of 45 degree, which could be eliminated by the pulse aging. After pulse aging, the new emission site on the 150 degree became dominant. The maximum field of 11.3 MV/m was achieved after the pulse aging. The  $Q_0$  at the field level was  $8.19 \times 10^8$ . The map at the maximum field shows the X-ray peaks on the 150 degree and 320 degree meridians (Fig.4(d)). But no heating spot was observed.

After one month later, the cavity was cooled again without any surface treatment. The cavity performance and the maps showed the same results as that of final state at the 1st cold test. The maximum Eacc and  $Q_0$  were 11.69 MV/m and  $8.8 \times 10^8$  respectively. The field was limited by the electron emission on the 150 degree and 320 degree (Fig. 4(e)), but the 45 degree did not appeared.

Warming up the cavity to room temperature did not affect to these emission sites. This suggests that the cause of the emission sites is not the gas condensation during cooling down but some defects on the surface.

#### 4. Development of HOM Absorber

The extracted HOM power is absorbed by the ferrite absorbers attached to the inner surface of the beam pipe. The high HOM power of 10 kW or more should be damped to the ferrite absorber. How to attach the ferrite on to the inner surface of the beam pipe is important. Three bonding methods have been tested; ultrasonic soldering, brazing and HIP (Hot Isostatic Press) [7]. The permittivity, permeability and out gassing rate of ferrite IB-004 in vacuum were measured.

#### 5. Input Coupler

The input coupler of the cavity should handle high RF power of 300 kW or more. We plan to use the almost same coupler as that for TRISTAN 5 cell superconducting cavities, that was tested upto 200kW [8], and that has a same ceramic window of 1 MW klystron. For the fundamental mode,  $Q_{ext}$  of input coupler was measured using the Al model cavity. The result shows that the  $Q_{ext}$  of higher than  $5 \times 10^4$  is available.

#### 6. Ozonized Ultrapure Water Treatment for Nb Surfaces

The X-ray maps at the maximum Eacc = 11.7 MV/m showed large electron emission at the whole area near the both irises of the cavity for the B-Factory. In order to get higher gradient, these electron emission have to be reduced. Stable, dense and thin Nb oxide layers on Nb surfaces can suppress the field electron and secondary electron emissions and photon stimulated desorption (PSD) from Nb surfaces. The surface work function for Nb surfaces is increased

from 4.0 to 5.9 eV by oxygen adsorption. Ozonized ultrapure water is a stronger and cleaner oxidizing agent than  $H_2O_2$  solution. Thick and porous oxide layers consisting of NbO,  $NbO_2$  and  $Nb_2O_5$  exist on the electropolished Nb surfaces. The weak superconductors like as NbO and  $NbO_2$  mixed layers on Nb surfaces have to be oxidized to dense and stable  $Nb_2O_5$  layers without any chemical residuals. The dense  $Nb_2O_5$  layers on Nb surfaces must be thinner than about some 10 Å thickness because thick oxide layers tend to include many micro-cracks.

In a super-clean room, the electropolished Nb samples were polished with ozone-added ultrapure water of three different concentrations (0.5, 2.0, 7.8 ppm) with flowing rate of 500 ml/min for 10, 20, or 30 min. After ozone treatments, the Nb surfaces were rinsed with ultrapure water for 10 min. The carbon contamination on the electropolished Nb surfaces, which was detected by the oil-free AES system using a dry pump and a turbomolecular pump, was removed completely by this ozone treatment (Fig. 5). The damping rates of O/Nb Auger peak height ratios by  $Ar^+$  sputtering for ozone treated Nb surfaces depend on polishing time rather than the ozone concentration. The preferential sputtering of oxygen by  $Ar^+$  beam does not occur for the dense amorphous  $Nb_2O_5$  films formed by longer ozone treatment (30 min). The PSD yield of synchrotron radiation light was reduced greatly for the ozone treated surface. The ozonized ultrapure water treatment can produce the clean, dense, stable and amorphous  $Nb_2O_5$  layers on Nb surfaces, which act as passive state to suppress the electron emission and PSD from the active Nb surfaces. We plan to apply this treatment to our B-Factory cavity.

## Acknowledgements

The authors would like to thank Prof. Y. Kimura, Prof. S. Kurokawa, Prof. E. Ezura and Prof. Emeritus Y. Kojima for their continuous encouragement and discussion. The fruitful discussions with other members of superconducting cavity group are greatly appreciated.

## References

- [1] Progress Report on Physics and Detector at KEK Asymmetric B-Factory, KEK Report 92-3, May, 1992.
- [2] H. Padamsee et al., "Superconducting RF Accelerating and Crab Cavities for the Cornell B-Factory, CESR-B", CLNS 90-1039, Laboratory of Nuclear Studies, Cornell University.
- [3] S. Mitsunobu et al., "Superconducting Cavity Development for KEK B-Factory" International Workshop on B-Factories (BFWS92), KEK, Tsukuba, Japan, 1992, p. 140
- [4] T. Takahashi et al., "Development of Superconducting Cavity for KEK B-Factory" Proc. of the 9th Symposium on Accelerator Science and Technology, KEK, Tsukuba, Japan, p. 327
- [5] T. Tajima et al. "Development of HOM absorber for KEK B-factory SC cavities",

this workshop.

- [6] S.Mitsunobu et. al. "Cryostat for TRISTAN Superconducting Cavity",Proc.of the 4th Workshop on RF Superconductivity,1989,KEK,Tsukuba,Japan,p 805
- [7] T.Tajima et.al. "Bonding of a Microwave-absorbing Ferrite,TDK IB-004,with Copper for the HOM Damper of the KEK B-Factory SC Cavities" ,this workshop.
- [8] S.Noguchi et.al. " Coupler-Experience at KEK" ,Proc.of the 4th Workshop on RF Superconductivity,1989,KEK,Tsukuba,Japan,p.397

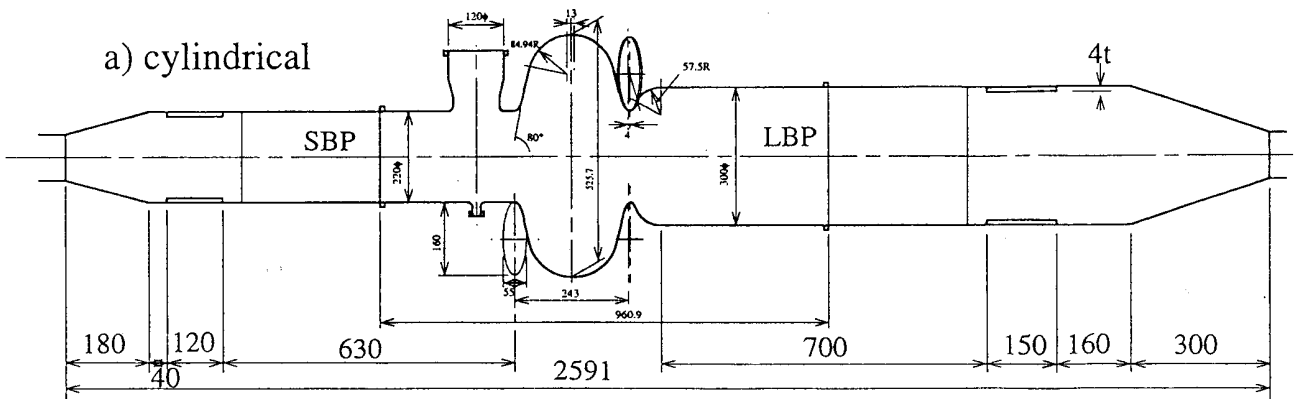


Fig.1 Optimized superconducting cavity shape for KEK B-Factory.

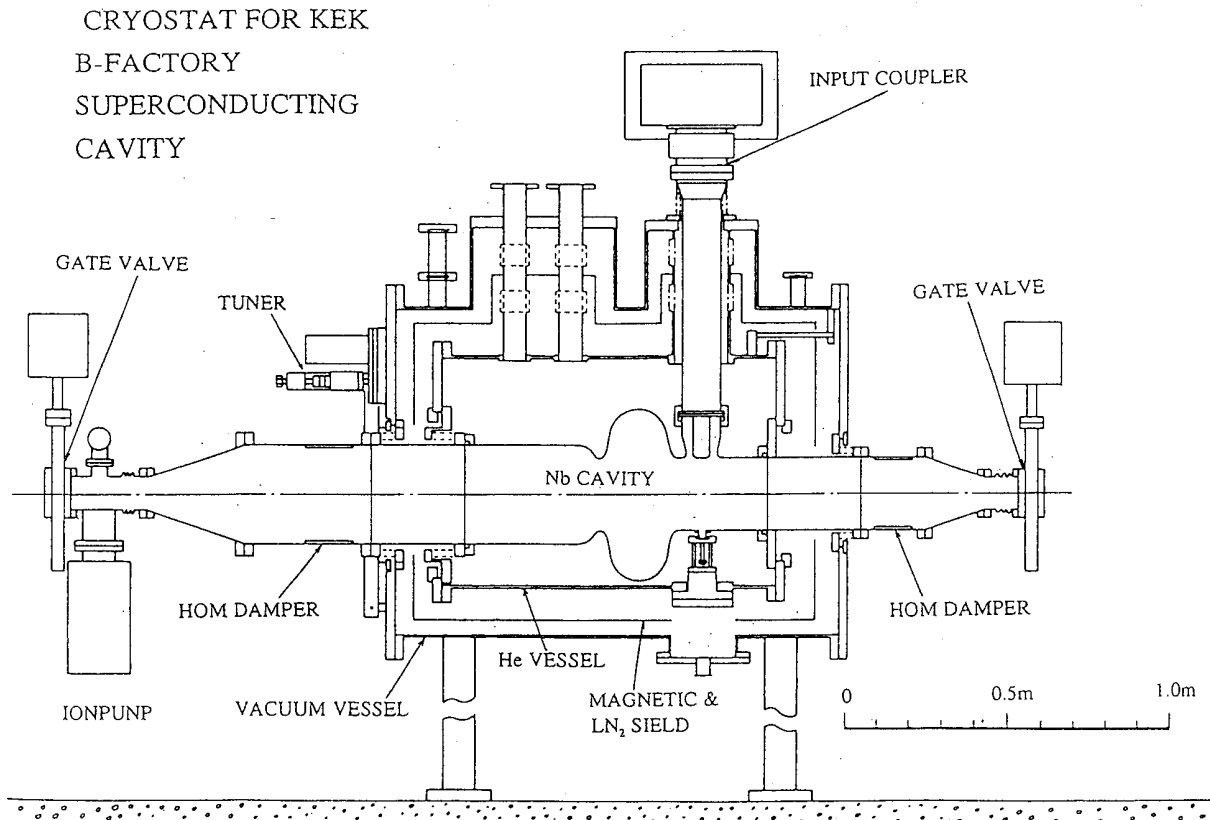


Fig. 2 AR beam test module with the optimized ferrite dampers.

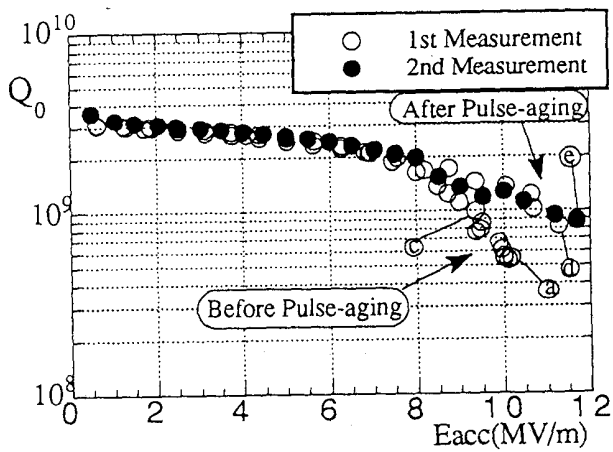


Fig. 3.  $Q_0$  vs  $E_{acc}$  for the cavity test at 4.2°K. The indexes of a,c,d,e are corresponding to Fig. 4 (a),(c),(d),(e) respectively.

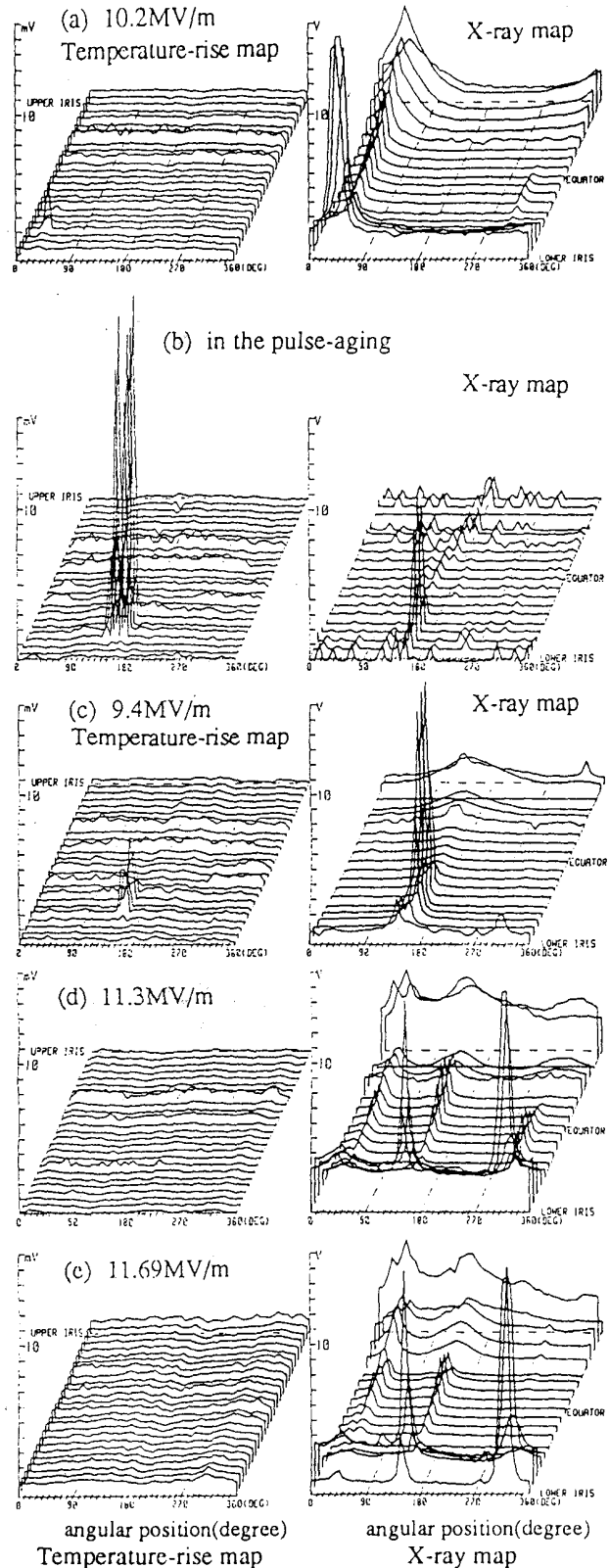


Fig. 4. Temperature-rise maps and X-ray maps, (a) after discharge, (b) in the pulse-aging, (c) after pulse-aging, (d) at just below  $E_{acc}$  max. of 1st measurement, (e) at just below  $E_{acc}$  max. of 2nd measurement.

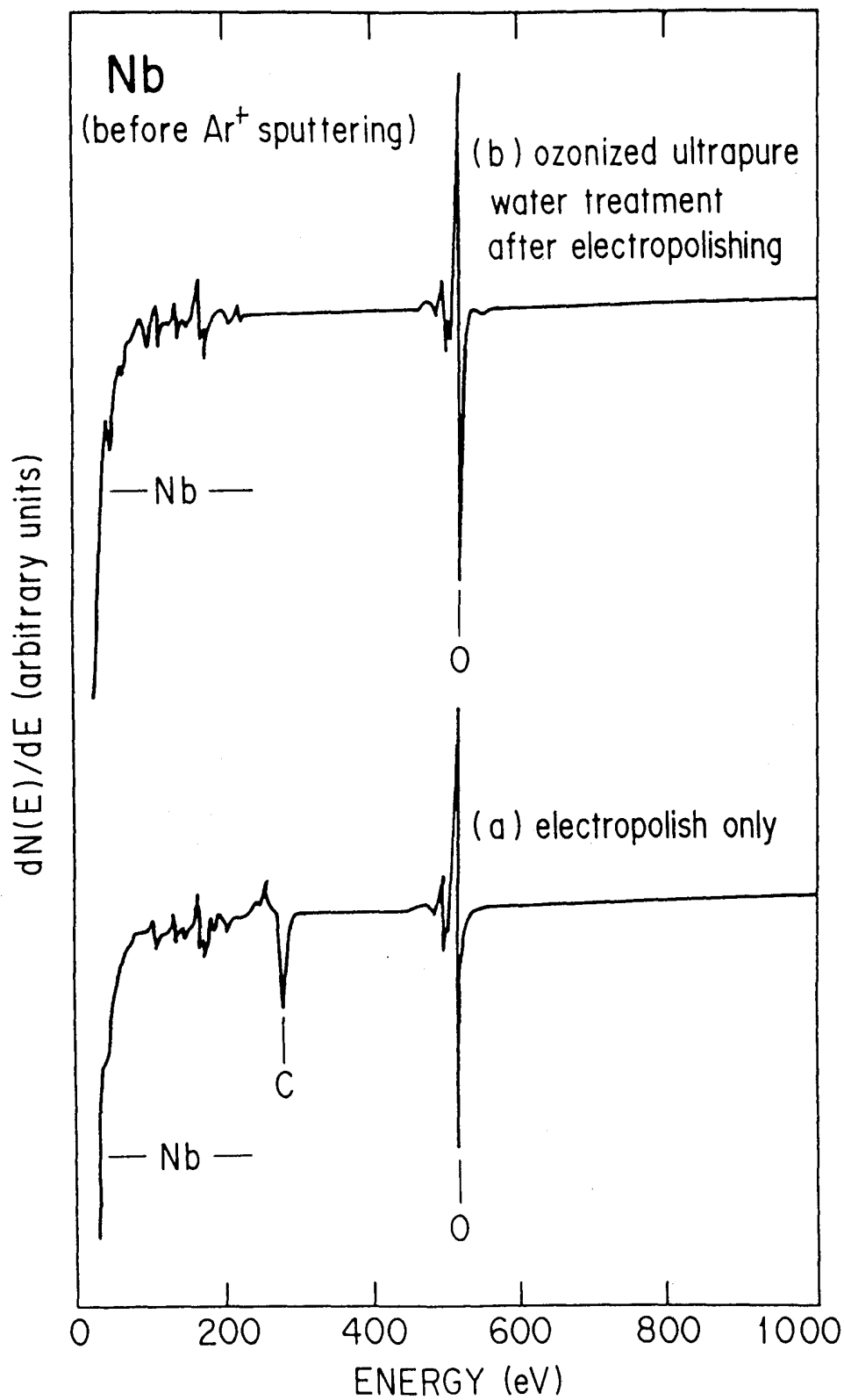


Fig. 5 Auger spectrum of Nb surfaces (a) electropolish only (b) ozonized ultrapure water treatment after electropolishing .